Spectroscopic investigations in ^{209}Bi I using tunable-cw-dye-laser spectroscopy

O. Poulsen* and J. L. Hall†

Joint Institute for Laboratory Astrophysics, University of Colorado and National Bureau of Standards, Boulder, Colorado 80309

(Received 24 March 1978)

Tunable-cw-dye-laser spectroscopy of an atomic-beam sample, combined with interferometric wavelength measurements, has been applied to the measurement of energy levels, hyperfine structure, and lifetimes of ^{209}Bi I. We find $E[(6p)^3\,^2P_{3/2}] = 33164.7000(7)$ cm^{-1}, $E[(6p)^2 7s\,^4P_{5/2}] = 48489.7593(8)$ cm^{-1}, and $E[(6p)^2 7s\,^2P_{3/2}] = 49460.8014(8)$ cm^{-1}. The hyperfine coupling constants A, B, are for the $(6p)^2 7s\,^4P_{5/2}$ level $(A, B) = [3717.4(5), -137.8(5.0)]$ MHz and for the $(6p)^2 7s\,^2P_{3/2}$ level $(A, B) = [2830.6(5), -132.6(4.6)]$ MHz. The lifetimes are determined to (5.25 ± 0.30) and (5.18 ± 0.20) ns, respectively.

I. INTRODUCTION

The spectrum of ^{209}Bi has been investigated intensively during the past 80 years, both experimentally and theoretically. Early experiments[1] established the splitting of the $(6p)^3$ ground configuration. This work was extended higher in resolution to resolve many hyperfine multiplets[2] belonging mainly to the $(6p)^3$ ground—and the $(6p)^2 7s$ configurations. In particular, the hyperfine structure (hfs) measurements were of importance in a theoretical understanding of complex spectra in intermediate coupling.[3]

More recently, the electromagnetic multipole character and strength of optical transitions within the $(6p)^3$ configuration have been of interest both theoretically[4] and experimentally.[5] Atomic-beam magnetic-resonance techniques (ABMR) have been used to measure very precisely the hyperfine structure of the lowest[6] $[^4S_{3/2}]$ and highest $[^2P_{3/2}](6p)^3$ levels.[7] Other previous Doppler-free measurements in Bi are level-crossing experiments[8] in the $(6p)^2 7s$ and $(6p)^2 6d$ configurations. Recently some optical measurements of modest resolution[9] have been analyzed for the hyperfine structure of $(6p)^2 7s$ as well as of several $(6p)^3$ levels: however, these results are in severe disagreement with the present Doppler-free precise optical results.

In spite of these works, and of other optical work using classical techniques such as grating and interferometric spectroscopy, the absolute energy levels, e.g., as compiled by Moore,[10] are quite uncertain even for levels in low-lying configurations.

For these reasons we have made precise sub-Doppler laser–atomic-beam measurements in ^{209}Bi. We report here three kinds of physical results: (i) absolute level positions of three levels of interest $[(6p)^3\,^2P_{3/2}$, $(6p)^2 7s\,^2P_{3/2}$, and $^4P_{5/2}]$, deduced with a fractional accuracy approaching 10^{-8} from the wavelength of the exciting laser; (ii) precise hyperfine structure splitting deduced from laser frequency-interval measurements; and (iii) accurate level lifetimes deduced from intensity-corrected linewidths.

II. APPARATUS AND EXPERIMENTAL METHODS

The method used in this work was tunable-cw-dye-laser spectroscopy of a collimated ^{209}Bi atomic beam, combined with absolute wavelength measurements of the dye laser, using an automatic scanning corner-cube interferometer.[11] Optical frequency intervals were measured with the aid of a stabilized high finesse Fabry-Perot etalon.

A. Atomic beam apparatus and detection

A conventional atomic-beam apparatus, consisting of an oven section, laser interaction section, and detection section was used (Fig. 1). The source of Bi atoms was a two-stage Mo oven described by Title and Smith.[6] A beam flux of $\sim 10^{12}$ particles/sec is obtained in the interaction region. The residual Doppler full width of the Bi beam is 14 MHz. In order to obtain a metastable $(6p)^3\,^2P_{3/2}$ beam, a coaxial cathode is placed in front of the snout of the oven (see Fig. 1). An emission of ~5 mA is sufficient to begin a dc discharge into the snout of the oven. Typically a discharge of 15 V, 300 mA at a Bi vapor pressure of 10^{-1} Torr optimizes the metastable content of the beam, monitored on the fluorescent light emitted subsequent to the laser excitation to the $(6p)^2 7s$ configuration. The fluorescence from the $(6p)^2 7s\,^2P_{3/2}$, $^4P_{5/2}$ levels is observed with a photomultiplier and an interference filter which passes only the resonance transitions at 2021 and 2060 Å, respectively (Fig. 2). The presence of metastable Bi atoms in the beam can also be detected using a Cs-coated surface via Auger electron emission. These electrons are detected with a channeltron multiplier. Time-of-flight velocity distributions were determined with the aid of pulsed excitation of the discharge or of an electron gun.

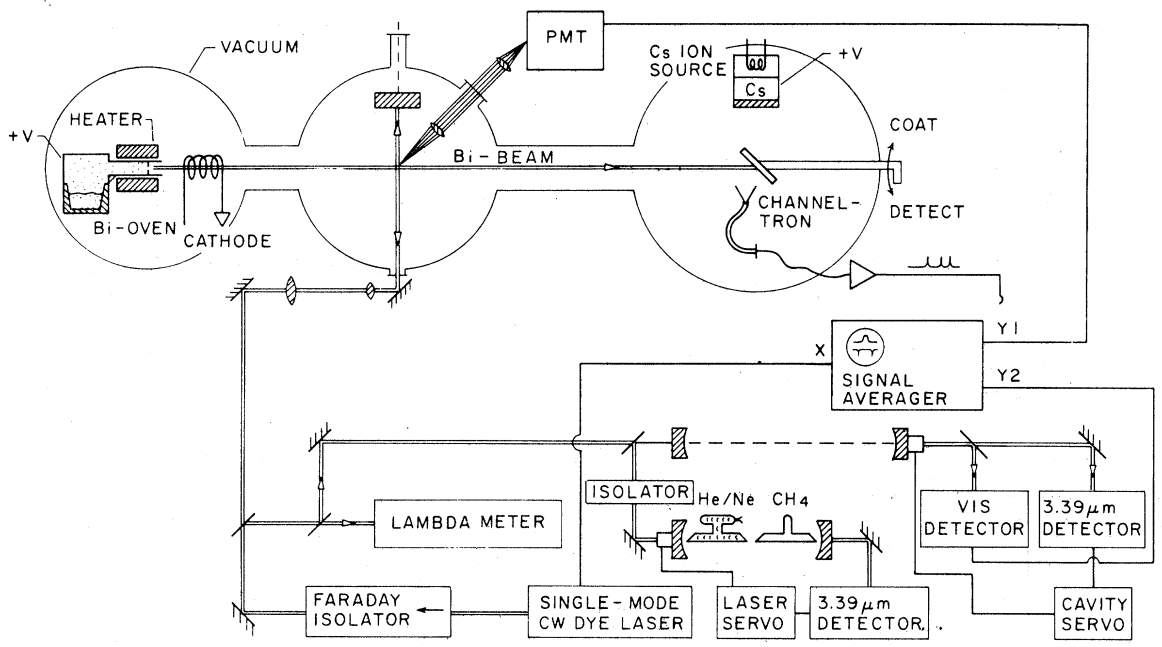

FIG. 1. Block diagram of experimental apparatus.

B. Laser and frequency determination

The optical transitions in Bi are induced by a tunable-cw-dye laser, which is actively stabilized onto a reference cavity. A continuous tuning range of 30 GHz, with a spectral width of ~2 MHz is available. The laser output power is in the range 30–100 mW depending on the dye and wavelength. The laser light is passed through the Bi beam at right angles. Figure 2 shows the transitions induced as well as their wavelengths.

To induce the transitions $(6p)^3\,^2P_{3/2}$-$7s\,^2P_{3/2}$,

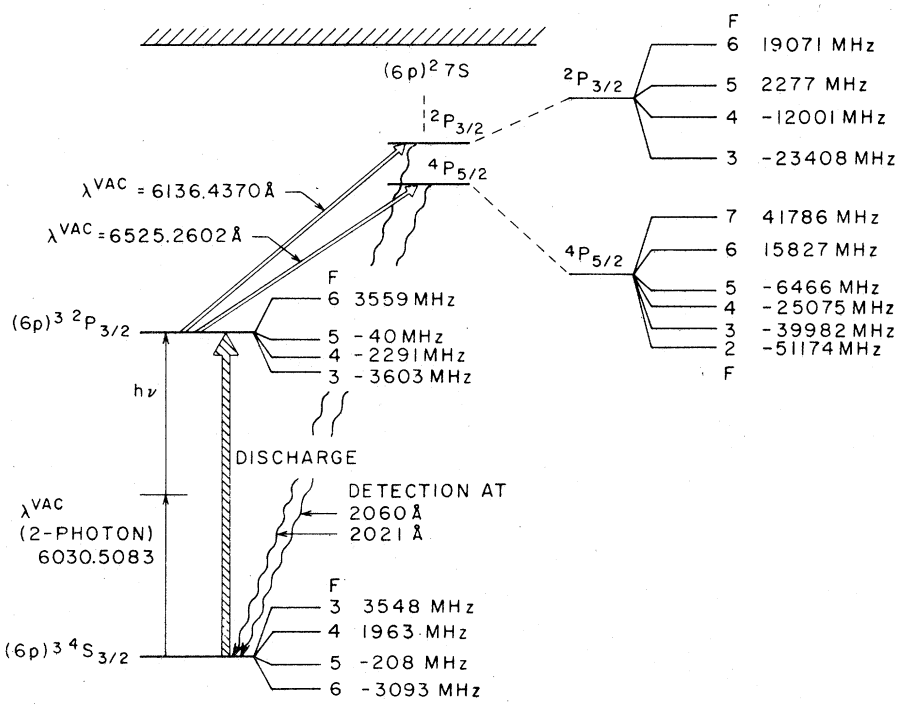

FIG. 2. Partial energy-level diagram of ^{209}Bi. Shown are the transitions induced as well as the measured hfs in the $7s\,^2P_{3/2}$, $7s\,^4P_{5/2}$ levels. The hfs of the $(6p)^3$ ground configuration is from Ref. 7.

$7s^4P_{5/2}$ the discharge was run to populate the metastable $(6p)^3\,^2P_{3/2}$. These metastable atoms traveled down the beam axis to the interaction region where the laser then easily excited these high-lying levels (Fig. 2). The dye-laser frequency was analyzed with a high finesse Fabry-Perot transfer cavity which was stabilized on the 3.39 μm output of a He-Ne laser. This He-Ne laser was in turn stabilized on the saturated absorption peak of the usual $F_2(2)$ Coriolis component of the $P(7)$ line in CH_4.[12] The transfer cavity then provides stable frequency marks, so that problems involving temperature drift of the dye laser, as well as nonlinearities in the frequency scan are essentially eliminated. The free spectral range of this Fabry-Perot was measured to 250.6 ± 0.1 MHz using a saturated absorption feature in ^{20}Ne.[13] This result is in complete agreement with an internal calibration using the $(6p)^3\,^2P_{3/2}$ hfs splitting. The fluorescent signal and the reference fringes are recorded simultaneously and stored in a multichannel averager. Linear interpolation is applied to deduce hfs line positions between two calibration fringes. Usually only a single sweep at 40 ms/channel was sufficient.

C. Wavelength determination

The wavelength of the power laser was measured with an automatic-scanning corner-cube interferometer (the "λ-meter").[11] The vacuum wavelength of the dye laser is related to the vacuum wavelength of the reference laser as follows

$$\lambda_v = (C/N)\,(\lambda_{\mathrm{ref,vac}}/100)\,[1+(n_\lambda - n_{\mathrm{ref}})/n_{\mathrm{ref}}]\,, \quad (1)$$

where N is the number entered into a preset counter, C is the counter reading of the λ-meter, and n_λ, n_{ref} are the indices of refraction. The wavelength of the reference laser was measured and the entire wavelength-measurement technique verified using two wavelength standards: (i) the Kr standard at 6057.8021 Å and (ii) a He-Ne laser stabilized on the B line of $^{129}I_2$ at 6329.90078 Å. The reference laser for the interferometer was a single-mode He-Ne laser frequency stabilized by comparing the power emitted in two orthogonal linear polarizations. In the krypton measurements, an Englehardt-type ^{86}Kr standard lamp was operated under the metrologically defined conditions ($J = 0.3$ A/cm^2, T is the triple-point temperature of N_2). Rather than observing the emitted light interferometrically, we focused the attenuated laser beam into the discharge capillary from the anode end. The Kr transition at 6057.8021 Å was monitored by observing the depletion of the discharge-populated $2p_{10}$ level when the laser was tuned over this resonance. This depletion was directly detectable via the decay $2p_{10}$-$1s_4$ at 9754 Å (Fig. 3). Observation of the λ-meter counter reading C for a given preset number N thus determines $\lambda_{\mathrm{ref,vac}}$ of the λ-meter reference laser. The value obtained in this case was

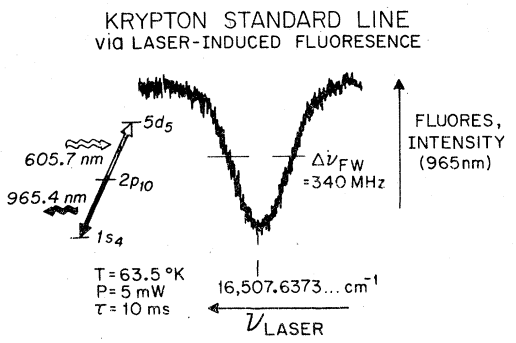

FIG. 3. Kr-standard line, observed via laser induced fluorescence.

$$\lambda_{\mathrm{ref,vac}} = 6329.9167(4)\ \text{Å}\,.$$

In another measurement, using the He-Ne laser, stabilized to the B line in $^{129}I_2$, the zero-frequency beat between the dye laser and this $^{129}I_2$ stabilized He-Ne laser was obtained. By measuring the wavelength of the dye laser $\lambda_{\mathrm{ref,vac}}$ was determined to be

$$\lambda_{\mathrm{ref,vac}} = 6329.9174(4)\ \text{Å}\,.$$

The small difference, although within the uncertainty limits, may reflect an influence of the time interval of two months as well as the unconventional use of the ^{86}Kr standard lamp. The calibrations were performed immediately after the two sets of Bi hfs measurements. The corrections due to local (p, T) were calculated with the Edlén index of refraction formula[14] using $p = 630$ Torr and $T = 25$ °C.

III. EXPERIMENTAL RESULTS

A. hfs intervals

The identification of the hyperfine spectra is simple, as the hfs splittings in the initial $(6p)^3\,^2P_{3/2}$ level are precisely known.[7] In Fig. 4 is shown a typical part of the spectrum of $(6p)^2 7s^2P_{3/2}$-$(6p)^3\,^2P_{3/2}$ excited around 6136.40 Å. The transition $(6p)^2 7s\,^4P_{5/2}$-$(6p)^3\,^2P_{3/2}$, excited around 6525.26 Å, which has not been previously reported in the literature was also readily obtained. In Table I are shown all experimentally measured hfs intervals, along with the initial-state splittings given by Landman and Lurio.[7] The data are averages of several sets of data, which were within ±4 MHz, identical. Doppler shifts due to misalignment

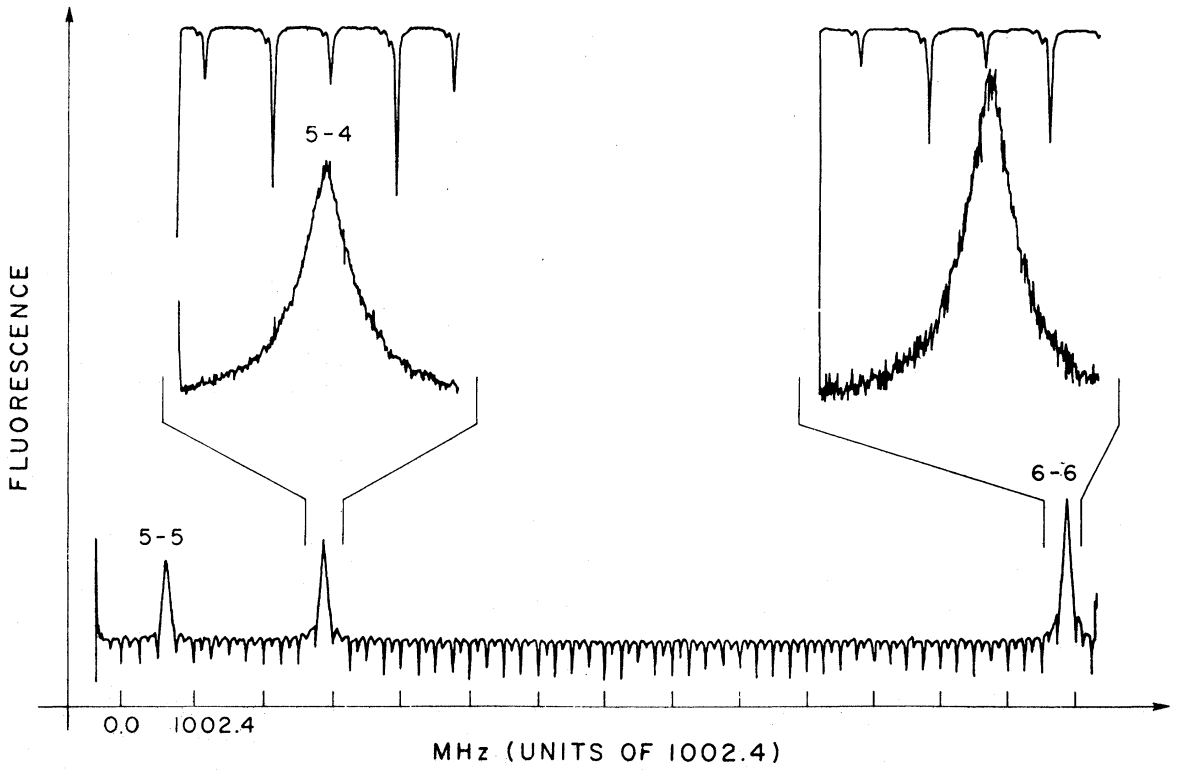

FIG. 4. Part of the hfs multiplet in the transition $(6p)^2 7s\ ^2P_{3/2}$-$(6p)^3\ ^2P_{3/2}$. The linewidth of the transitions corresponds to $I = 9.2 I_0$, thus showing a drastic power broadening of the lines. No frequency shifts were experimentally observed for $0.023\ I_0 < I < 21.5\ I_0$. Recording time was 5 sec. The downward-going-Fabry-Perot calibration resonances have a spacing of 250.6 MHz.

TABLE I. Experimental observed hfs multiplet splittings in $(6p)^2 7s\ ^2P_{3/2}$ and $^4P_{5/2}$. Also shown are the precise splittings of the $(6p)^3\ ^2P_{3/2}$, measured by Landman and Lurio (Ref. 7).

Interval $E(F\text{-}F')\text{-}E(F''\text{-}F''')$	$(6p)^2 7s\ ^2P_{3/2}$ Splitting (MHz) (± 4 MHz)	Splitting of $(6p)^3\ ^2P_{3/2}$ (Ref. 7)
4-3, 5-6	7 021	
5-6, 5-4	5 852	5 850
3-4, 3-3	1 310	1 312
3-3, 4-5	7 847	
4-5, 4-3	3 564	3 564
5-4, 6-6	11 042	
5-6, 5-5	3 598	3 599
5-5, 5-4	2 254	2 251
6-6, 6-5	3 597	3 599
Interval $E(F\text{-}F')\text{-}E(F''\text{-}F''')$	$(6p)^2 7s\ ^4P_{5/2}$ Splitting (MHz) (± 4 MHz)	Splitting of $(6p)^3\ ^2P_{3/2}$ (Ref. 7)
7-6, 6-5	22 360	
6-6, 6-5	3 601	3 599
5-4, 6-6	16 444	
5-5, 5-4	2 249	2 251
4-4, 5-5	16 359	
3-3, 4-4	13 591	
2-3, 3-3	11 186	
4-3, 4-4	1 312	1 312

TABLE II. Observed vacuum wavelengths λ^{vac} for hfs transitions $(6p)^2 7s\ ^2P_{3/2}$-$(6p)^3\ ^2P_{3/2}$ and $(6p)^2 7s\ ^4P_{5/2}$-$(6p)^3\ ^2P_{3/2}$.

Transition	λ^{vac} (Å)
$(6p)^2 7s\ ^2P_{3/2}$	
5-4	6136.3805(2)
6-5	6136.1971
3-3	6136.6854
4-3	6136.5423
3-4	6136.7022
5-6	6136.4536
4-5	6136.5865
5-5	6136.4089
6-6	6136.2418
$(6p)^2 7s\ ^4P_{5/2}$	
7-6	6524.7174(2)
6-6	6525.0860
5-5	6525.3514
5-4	6525.3184
4-4	6525.5834
3-3	6525.7766
2-3	6525.9349

were negligible, as was also verified experimentally by the use of a retroreflector.

B. Wavelengths

The wavelengths of all the observed hfs transitions for the $(6p)^2 7s^4P_{5/2}$-$(6p)^3\ ^2P_{3/2}$ and $(6p)^2 7s^2P_{3/2}$-$(6p)^3\ ^2P_{3/2}$ hfs multiplets are listed in Table II. Furthermore, in order to measure the absolute energy levels, the wavelengths of the two-photon transitions $(6p)^3\ ^2P_{3/2}$-$(6p)^3\ ^4S_{3/2}$ were measured for three hfs components.[15] These weak transitions were detected by impact Auger electron emission by metastable atoms produced by laser, rather than discharge excitation. The observed transitions are listed in Table III. The uncertainties in these wavelength measurements are ±0.0004 Å corresponding to ±32 MHz. This includes statistical scatter of the data (~8 MHz) as well as systematic errors in the calibration and alignment of the λ-meter.

C. Lifetimes

The lifetimes of the short-lived states $7s\ ^2P_{3/2}$, $7s\ ^4P_{5/2}$ can be deduced from an analysis of the observed hfs-line profiles. The expected linewidth FWHM as a function of laser intensity is given by[16]

$$w = w_0(1 + I/I_0)^{1/2}, \qquad (2)$$

where w_0 is the halfwidth due to natural decay in zero intensity, I is the laser intensity, and I_0 the intensity required for a saturation parameter of 1. In Fig. 5 are shown a set of hfs profiles obtained at different laser powers I for the $7s\ ^2P_{3/2}$ level. In order to extract the natural halfwidths w_0, these profiles are least-squares fitted to a Lorentzian with halfwidth w convoluted with a Gaussian of 14 MHz fullwidth, representing the beam Doppler profile. For transitions to the $7s\ ^2P_{3/2}$ level, the laser intensity I was varied ×1000 as strong saturation was observed. As may be seen from the inset in Fig. 5, the experimental linewidths are in good agreement with the expected functional dependence, Eq. (2). I_0 was determined to be 1.32W/cm² for this transition $[7s\ ^2P_{3/2}$-$(6p)^2\ ^2P_{3/2}]$. It is clear that oscillator strength information is contained in the parameter I_0, but in the present experiments analysis would be difficult since the laser mode radius of 170 μm is substantially less

TABLE III. Observed vacuum wavelengths λ^{vac} for hfs transitions $(6p)^3\ ^2P_{3/2}$-$(6p)^3\ ^4S_{3/2}$ measured in two-photon absorption.

Transition	λ^{vac} (Å)
6-6	6030.4678(1)
5-5	6030.5067
4-4	6030.5337

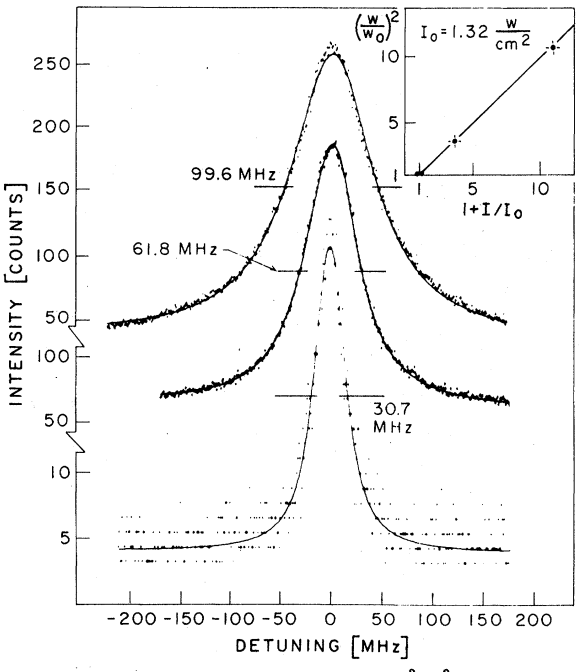

FIG. 5. The 6-6 hfs component in $(6p)^2 7s\ ^2P_{3/2}$ as function of laser intensity. The natural width (FWHM), after deconvoluting the Bi-beam Doppler profile is $w_0 = 30.7 \pm 1.0$ MHz for laser powers $I \ll I_0$. Shown also are the extrapolation of w_0 to zero laser power.

than the height of the atomic beam (≈1 mm). Choice of a more suitable geometry and extension of the theory to include spatial inhomogeneity would make this interesting possibility more realistic.

IV. DISCUSSION

A. hfs results

In the $(6p)^2 7s$ configuration the hfs are reasonably small, so that only a negligible mixing between different J states is present. Thus J remains a good quantum number. The hfs Hamiltonian is given by

$$\hat{\mathcal{H}}_{\rm hfs} = A\hat{I}\cdot\hat{J} + B\left[\frac{\frac{3}{2}\hat{I}\cdot\hat{J}(2\hat{I}\cdot\hat{J}+1) - I(I+1)J(J+1)}{2I(2I-1)J(2J-1)}\right] \tag{3}$$

for the diagonal interactions. I is the nuclear spin of ^{209}Bi. A and B are the magnetic dipole and the electric quadrupole interaction constants, respectively. Thus the energy of a $|\alpha JIFM_F\rangle$ state is given by

$$W_F = \tfrac{1}{2}AK + B\,\frac{3K(K+1) - 2I(I+1)2J(J+1)}{4I(2I-1)2J(2J-1)} + W_F^{(2)}, \tag{4}$$

where

$$K = F(F+1) - I(I+1) - J(J+1)$$

and

$$W_F^{(2)} = \sum_{\alpha' J'} \frac{|\langle \alpha JFM_F|\hat{\mathcal{H}}_{\rm hfs}|\alpha' J' FM_F\rangle|^2}{W(\alpha J) - W(\alpha' J')} \tag{5}$$

is the second-order energy contribution due to neighboring fine-structure levels, that is $\alpha J \neq \alpha' J'$. The matrix elements contributing to $W_F^{(2)}$ are given by Childs[17] for configurations l^N and $l^N l'$, in terms of the one-electron parameters $a^{k_1 k_2}$, $b^{k_1 k_2}$ of Sandars and Beck.[18] These parameters are directly related to the measured A and B values of the levels in the $(6p)^2 7s$ configuration and their wave functions in intermediate coupling. The dominant contributions to $W_F^{(2)}$ stem from the interaction between the $7s\,^2P_{3/2}$ and the $7s\,^4P_{5/2}$ levels only separated approximately 968 cm^{-1}. Thus we get the following expressions for the observed hfs splittings for the $(6p)^2 7s\,^2P_{3/2}$ and $^4P_{5/2}$ levels, respectively, including the contributions from $W_F^{(2)}$ (in MHz):

$$\begin{aligned} W_{6,5} &= 6A + \tfrac{2}{3}B - 0.6, \\ W_{5,4} &= 5A - \tfrac{5}{24}B + 0.6, \\ W_{4,3} &= 4A - \tfrac{2}{3}B + 1.1, \end{aligned} \tag{6}$$

$$\begin{aligned} W_{7,6} &= 7A + \tfrac{7}{15}B + 2.3, \\ W_{6,5} &= 6A + \tfrac{3}{40}B + 0.6, \\ W_{5,4} &= 5A - \tfrac{1}{6}B - 0.6, \\ W_{4,3} &= 4A - \tfrac{17}{60}B - 1.1, \\ W_{3,2} &= 3A - \tfrac{3}{10}B - 1.2, \end{aligned} \tag{7}$$

Fittings Eqs. (6) and (7) to the experimental data in Tables I and II, respectively, the following values for the magnetic dipole and electric quadrupole interaction constants A and B are found

$$\left.\begin{aligned} A &= 2830.6 \pm 0.5 \text{ MHz} \\ B &= -132.6 \pm 4.6 \text{ MHz} \end{aligned}\right\} 7s\,^2P_{3/2}$$

$$\left.\begin{aligned} A &= 3717.4 \pm 0.5 \text{ MHz} \\ B &= -137.8 \pm 5.0 \text{ MHz} \end{aligned}\right\} 7s\,^4P_{5/2}.$$

The uncertainties quoted include: (i) statistical scatter of the fitted A, B values, (ii) an uncertainty of 0.1 MHz on the calibration of the transfer cavity free spectral range of 250.6 MHz, and (iii) an error, amounting to a maximum of ±3 MHz in applying a linear interpolation between two Fabray-Perot cavity orders of 250.6 MHz. It is worth noting that the precise splittings of the $(6p)^3\,^2P_{3/2}$ initial state, measured by Landman and Lurio[7] are very well reproduced in this work, the largest difference being 3 MHz.

In Table IV are compared several measurements of hfs in the $(6p)^2 7s$ configurations of ^{209}Bi. The works of Mrozowski[2] and Dembczyński *et al.*[9] employ classical spectroscopic techniques. Their

TABLE IV. Experimental A, B values (in MHz) for the $^2P_{3/2}$, $^4P_{5/2}$ states of the $(6p)^2 7s$ configurations.

	$7s\,^2P_{3/2}$		$7s\,^4P_{5/2}$	
	A	B	A	B
This work	2830.6 ± 0.5	−132.6 ± 4.6	3717.4 ± 0.5	−137.8 ± 5.0
Dembczyński *et al.* (Ref.9)	2830.9 ± 1.2	−30 ± 6	3733.3 ± 2.1	−101.9 ± 30.0
Mrozowski (Ref. 2)	2857	−60	3732	−87

TABLE V. Experimentally determined energy levels (in cm^{-1}).

Level	Energy (cm^{-1}) (this work)	Energy (cm^{-1}) (Ref. 10)
$(6p)^3\,^2P_{3/2}$	33 164.7000 ± 0.0007 [a]	33 164.84
$(6p)^2 7s\,^4P_{5/2}$	48 489.7593 ± 0.0008	48 489.88
$(6p)^2 7s\,^2P_{3/2}$	49 460.8014 ± 0.0008	49 461

[a] Reference 15.

resolution was instrumentally limited to approximately 1700-MHz FWHM in the best cases, thus creating problems due to heavily overlapping lines. In our dye-laser–atomic-beam work, with the calibration interferometer directly stabilized by the CH_4-stabilized laser, the useful resolution is essentially limited only by the natural linewidth for the levels investigated.

The electric quadrupole interaction constant B depends, in $l^N l'$ configurations, only on two parameters, b^{02}_{6p} and b^{11}_{6p}.[17] In order to determine b^{02}_{6p} and b^{11}_{6p} a good knowledge of the eigenvectors in intermediate coupling is required in addition to precise values for B for two levels in the configuration. Using the eigenvectors similar to those of Ref. 4, which take into account the spin-orbit and the electrostatic interactions, only rough estimates of b^{02}_{6p} and b^{11}_{6p} can be made. The reason is that such eigenvectors only represent the actual energy levels in the $(6p)^2 7s$ configuration to within ~2%. Improved hfs calculations will thus make configuration interaction wave functions necessary. Severe configuration interaction might be expected from the $6s6p^4$ and $6s^2 6p^2 6d$ configurations, but the present work does not attempt to calculate such interactions or to improve them by introducing other magnetic interactions within the configuration.[19] Nevertheless, the present experimental B values for the $(6p)^2 7s\,^2P_{3/2}$ and $(6p)^2 7s\,^4P_{5/2}$ levels clearly show the need for a better understanding of the interactions in the $(6p)^2 7s$ configuration and its interaction with other configurations.

B. Wavelengths and energy levels

Using the known hfs of the $(6p)^3\,^2P_{3/2}$ level[7] and the A, B values (Table IV) measured in this work, the center of gravity (c.g.) energy levels for the $(6p)^3\,^2P_{3/2}$ and $(6p)^2 7s\,^2P_{3/2}$, $^4P_{5/2}$ levels can be precisely determined from the wavelength measurements of Tables II and III. In Table V are shown the experimentally determined energy levels together with the data compiled and calculated by Moore.[10] The present energy-level data, with a total uncertainty of ±50 MHz, clearly show that in high-resolution spectroscopic work, in particular with Doppler-free techniques, and resonance widths on the order of a few MHz, the energy-level tables[10] are not sufficiently precise. In the present case of bismuth, we find that these energy values may be inaccurate by far more than the apparent uncertainty, some $+14\sigma$ in the case of the metastable $^2P_{3/2}$ level. With the present laser techniques many atoms (and molecules) could be investigated in order to provide precise wavelength data and thus yield improved values over the published energy levels.

C. Lifetimes

In the present work lifetimes have been measured using selective laser excitation to a specified hyperfine level. For one of the multiplets discussed, $(6p)^2 7s\,^4P_{5/2}$, the lifetime has been precisely measured using the Hanle effect subsequent to excitation of a Bi vapor with a Bi resonance lamp.[20] Also both levels have been measured using the beam-foil technique.[21] In Table VI all the measured lifetimes are shown. For the $7s\,^4P_{5/2}$ level good agreement is found between the Hanle-effect measurement, this work, and the beam-foil result. (The latter technique produces nonselective excitation and thus can be affected by cascade.) For the $(6p)^2 7s\,^2P_{3/2}$ level agreement between the beam-foil result and the present result is, within the uncertainty levels, good.

V. CONCLUSION

This work shows the not surprising result that the spectroscopy of the ^{209}Bi I spectrum needs a great deal of attention before it can be fully understood. The precise hfs measurements clearly indicate the need for a careful calculation based on improved configuration interaction wave functions, in spite of the difficulty of such an under-

TABLE VI. Lifetimes (in ns) for the $^2P_{3/2}$, $^4P_{5/2}$ states of the $(6p)^2 7s$ configuration.

	Method	$7s\,^4P_{5/2}$	$7s\,^2P_{3/2}$
This work	Laser–A Beam	5.25 ± 0.30	5.18 ± 0.20
Anderson[21]	Beam foil	5.5 ± 0.5	4.8 ± 0.4
Svanberg[20]	Hanle effect	4.9 ± 0.25	

taking. Also the wavelength measurements, yielding energy levels, demonstrate the necessity of interest in the optical spectroscopy of heavy atoms in order to meet the needs of high-resolution Doppler-free spectroscopy techniques. In turn such techniques might, as in this case, provide such basic information. The measured lifetimes, which are in excellent agreement with Hanle-effect and beam-foil measurements, indicate that this technique may be used to provide reliable lifetimes, in the cases for which selective optical excitation is possible. Performing optical Zeeman spectroscopy or Hanle-effect measurements on the laser excited states, would yield g_J and g_F values, as the lifetimes already are determined, and thus provide further information concerning possible configuration interactions.

ACKNOWLEDGMENTS

The authors have benefited from discussions with colleagues J. C. Bergquist and S. A. Lee. One of the authors (O.P.) acknowledges support from the Danish National Science Research Council. We also thank A. Lurio for discussion of the Auger metastable atom detector. The work was supported in part by the NSF under Grant No. PHY76-04761 to the University of Colorado and in part by the National Bureau of Standards as part of its programs on improved precision measurements for application to basic standards.

---

*Permanent address: Institute of Physics, University of Aarhus, DK8000 Aarhus C. Denmark.

†Staff member, Quantum Physics Division, National Bureau of Standards.

[1]V. Thorsen, Z. Phys. 40, 642 (1926).

[2]S. Mrozowski, Phys. Rev. 62, 526 (1942); P. Zeeman, E. Back, and S. Goudsmith, Z. Phys. 66, 1 (1930).

[3]G. Breit and L. A. Wills, Phys. Rev. 44, 70 (1933).

[4]R. H. Garstang, J. Res. Nat. Bur. Stand. Sect. A 68, 61 (1964).

[5]J. Heldt, J. Opt. Soc. Am. 58, 1516 (1968); S. T. Dembinski, J. Heldt, and L. Wolniewicz, *ibid.* 62, 555 (1972); L. Augustyniak, J. Heldt, and J. Branowski, Phys. Scr. 12, 157 (1975).

[6]K. S. Title and K. F. Smith, Philos. Mag. 5, 1281 (1969); R. J. Hull and G. O. Brick, Phys. Rev. A 1, 685 (1970).

[7]D. A. Landman and A. Lurio, Phys. Rev. A 1, 1330 (1970).

[8]L. Holmgren and S. Svanberg, Phys. Scr. 9, 211 (1974).

[9]J. Dembczyński and M. Frackowiak, Acta Phys. Pol. A 48, 139 (1975); J. Dembczyński, B. Arcimowicz, and K. Wisniewski, J. Phys. B 10, 2951 (1977).

[10]C. Moore, "Atomic Energy Levels," NSRDS-NBS 35, Vol. III (1971).

[11]J. L. Hall and S. A. Lee, Appl. Phys. Lett. 29, 367 (1976).

[12]J. Hall, in *Colloques Internationaux du C.N.R.S.*, No. 217 (Paris, 1974), pp. 105–125.

[13]J. Bergquist, Ph.D. thesis (University of Colorado, 1978) (unpublished).

[14]*American Institute of Physics Handbook*, edited by D. E. Gray (McGraw-Hill, New York, 1963), 2nd ed., pp. 6–96.

[15]J. L. Hall, O. Poulsen, S. A. Lee, and J. C. Bergquist, J. Opt. Soc. Am. 68, 697 (1978).

[16]M. Sargent III, M. O. Scully, and W. E. Lamb, Jr., *Laser Physics* (Addison-Wesley, Reading, MA., 1974).

[17]W. J. Childs, Phys. Rev. A 2, 316 (1970).

[18]P. G. H. Sandars and J. Beck, Proc. R. Soc. London A 289, 97 (1965).

[19]S. Obi and S. Yanagawa, Publ. Astron. Soc. Jpn. 7, 125 (1955).

[20]S. Svanberg, Phys. Scr. 5, 73 (1972).

[21]T. Andersen, O. Madsen, and G. Sørensen, J. Opt. Soc. Am. 62, 1118 (1972).